Research Article | Vol. 2, No. 1 | 15 Jan 2019 | OSA CONTINUUM 184
OSA CONTINUUM

Diode pumped cw ruby laser

W. LUHS[1,*] AND B. WELLEGEHAUSEN[2]

[1]Photonic Engineering Office, Herbert-Hellmann-Allee 57, 79189 Bad Krozingen, Germany
[2]Institut für Quantenoptik, Leibniz Universität Hannover, Welfengarten 1, 30167 Hannover, Germany
*luhs@luhs.de
https://luhs.de

Abstract: Cw laser oscillation of ruby at 694 nm in linear and ring resonators is reported for the first time, pumped with a 1 W laser diode at 405 nm as well as 445 nm. The ruby laser operates at room temperature with a threshold of 200 mW at 405 nm and 400 mW at 445 nm. So far output powers up to 36 mW have been achieved pumped at 405 nm. With the ruby ring laser highly coherent single frequency operation will be possible.

1. Introduction

In 1960 T. Maiman realized the first laser [1], the ruby laser, which started a tremendous and ongoing development of laser sciences and optical technologies. The ruby laser operates at wavelengths of 694.3 nm (R1 line) and 692.8 nm (R2 line), corresponding to transitions between Cr^{3+} ions (Fig. 1), embedded in the host crystal Al_2O_3 (aluminum oxide). Unfortunately, this laser is difficult to operate, as it uses a three level scheme and needs population inversion with respect to a strongly populated ground state. The ruby laser remained the only three level laser system with inversion to the ground state, while all other lasers developed later on use laser transitions between excited states in a four level scheme. To operate ruby, typically fast flash

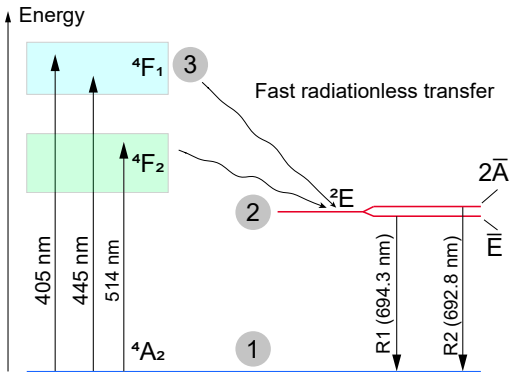

Fig. 1. Ruby energy level diagram (after Ref. [2]). Indicated are the three relevant levels

lamp pumping is applied, making use of the broad absorption bands (Fig. 1) and the long lifetime of the upper laser level of about 3.5 ms, which allows storing of population. Consequently, the ruby laser has mostly been used for high energy pulse laser applications. However, considering rate equation calculations, cw operation is not forbidden, but requires intense pumping and specific conditions. In fact, cw operation has been reported, using pumping with a mercury arc lamp [3, 4] or a cw argon ion laser at 514 nm [5–7] and other refs. therein. However, in most of these investigations cooling of the ruby rod to liquid nitrogen temperature was applied, which decreases the fluorescence line width by about a factor of 70 with respect to room temperature [8], and leads to a corresponding reduction of the pump intensity requirements.

#351844 https://doi.org/10.1364/OSAC.2.000184
Journal © 2019 Received 13 Nov 2018; accepted 12 Dec 2018; published 8 Jan 2019

OSA CONTINUUM

Most attractive today surely is laser pumping using available powerful laser diodes. To realize conditions for cw operation at room temperature, a factor of about 70 gained by the cooling to liquid nitrogen temperature has to be compensated. This is more than possible by pumping at the optimum of the absorption profile at 405 nm [9] and by the use of low loss adequate optical resonators. Due to the narrow and Doppler free line width of the ruby laser emission, a compact highly coherent system should thus be possible. Cw operation was achieved by pumping with laser diodes at 405 nm and 445 nm. Here we report on first detailed investigations of a cw ruby laser pumped with a 1W laser diode at 405 nm. By strong focusing into a 8.6 mm AR coated ruby rod and using a semi-concentric optical resonator, we could achieve cw laser operation at room temperature with a threshold of about 200 mW (about 400 mW with 445 nm) and a maximum output of so far 36 mW. For the first time cw ruby ring laser operation is reported. Investigations on the operation conditions and features will be presented and possible applications will be discussed.

2. Experimental results

2.1. Linear resonator

Fig. 1 shows the level scheme relevant for the ruby laser. For pumping of the upper laser levels 2, two absorption bands $^4F_1$ and $^4F_2$ with maxima at 405 nm and 555 nm may be used [9].

According to [9], pumping at 405 nm with a laser diode is about a factor of 3 more effective than pumping with the 514 nm line from an argon ion laser.

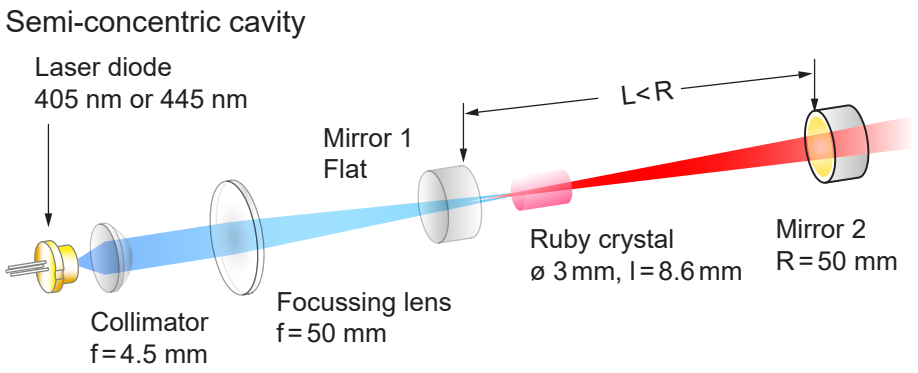

Fig. 2. Experimental setup of the semi-concentric resonator

The experimental setup is shown in Fig. 2. It consists of a 1 W diode at 405 nm (USHIO HL40033G) and a ruby within the semi-concentric resonator. The output of the diode is collimated with a f = 4.5 mm lens and then focused with an f = 50 mm lens through the flat mirror M1 (high reflectivity at 694 nm, transmission at 405 nm about 90%) into the ruby crystal (length 8.6 mm, diameter 3 mm, Cr_2O_3 concentration about 0.05 %, c-axis 90° to crystal axis), which has a broadband AR coating (<0.2% at 694 nm and 3% at 405 nm) on both flat sides. The crystal is placed close to the flat mirror and held in a collet chuck with no active cooling. The mirror M2 with radius of curvature R = 50 mm is placed at a distance L < R. For low threshold operation the mirror M2 has a high reflectivity coating for 694 nm and 405 nm. The high reflectivity at 405 nm simplifies the alignment and control of the distance L. By proper focusing of the pump radiation into the ruby crystal (see discussion below) laser oscillation starts at a threshold pump power of 200 mW. The Fig. 3 shows the laser line spectrum of the pump as well as the ruby laser. The spectrum has been recorded with a spectrometer with a resolution of 1 nm. We notice that the ruby laser oscillates simultaneously on both R lines. Of special importance is the dynamical

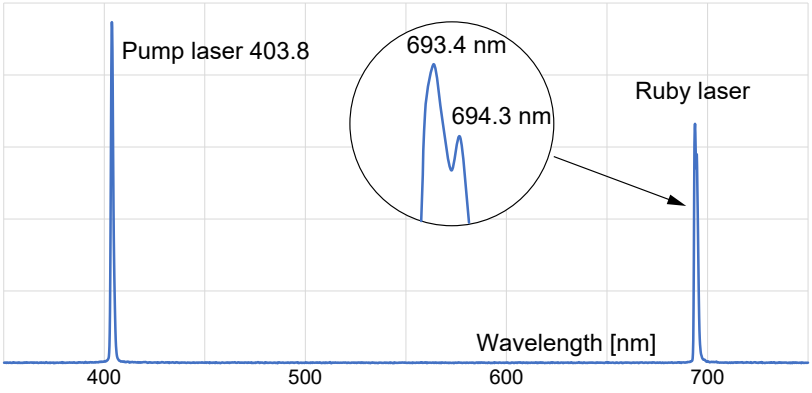

Fig. 3. Spectrum of the pump and ruby laser. Pump power 1W

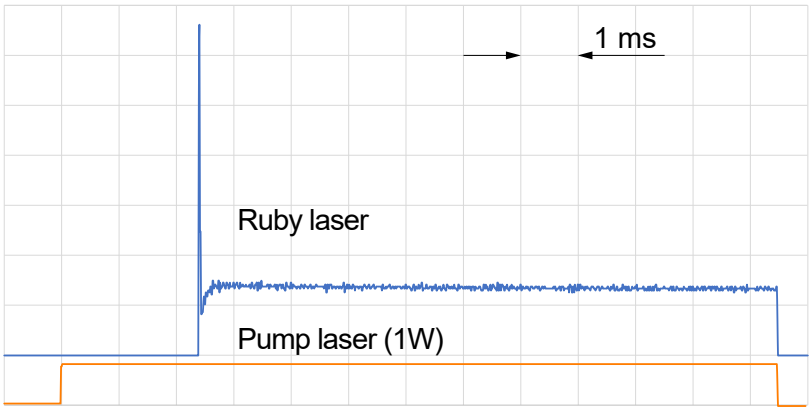

Fig. 4. Transient response of the ruby laser. Oscilloscope trace, similar to the observation of [5]

behavior of the ruby laser oscillation. In the early papers strong spiking and no real cw emission was reported [7]. To study this, the pump laser controller is set from cw to periodic on and off switching of the pump laser diode. The Fig. 4 shows the time dependence of the ruby laser emission and the corresponding power of the pump laser. The emission of the ruby laser was detected by a fast SiPIN photodiode (BPX61) with an amplifier having a 3dB cut-off frequency of 140 MHz. The time scale of the oscilloscope is set to 1 ms per division. The ruby laser starts with a delay of 2.3 ms. After the initial spiking, which is typical for lasers with a long lifetime of the laser level, the ruby laser oscillation reaches the steady state and operates as cw laser without spiking. The residual small fluctuations are due to external disturbances of the open structure of the ruby laser setup and due to transverse and hole burning mode competition.

To achieve lasing, a careful positioning of the ruby crystal with respect to the focusing lens is necessary. A change of the crystal position along the optical axis changes the radially emitted intensity as well as the fluorescence track inside the crystal (Fig. 5). At the optimum position a sharp narrow fluorescence track is observed with a minimum of radial fluorescence (Fig. 5 B). Deviations to longer or shorter distances to the focusing lens result in a diffuse fluorescence track and a noticeable stronger radial fluorescence. This can be seen in Fig. 5 A and C. We explain this behavior by the strong reduction of the refractive index (depletion of the ground state population) in the center of the pump beam, leading to a "channel" which guides and concentrates

OSA CONTINUUM

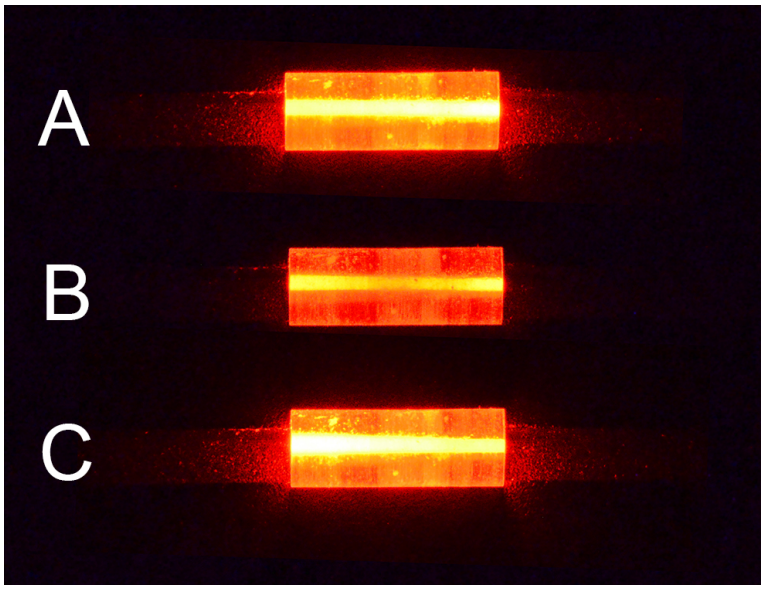

Fig. 5. Fluorescence tracks within the ruby crystal (L = 8.6 mm). (B) at optimum position, (C) at shorter and (A) at larger distance to focusing lens (f = 50 mm).

the fluorescence in the optimum position (see also discussions in [7]). Fig. 6 now gives the output

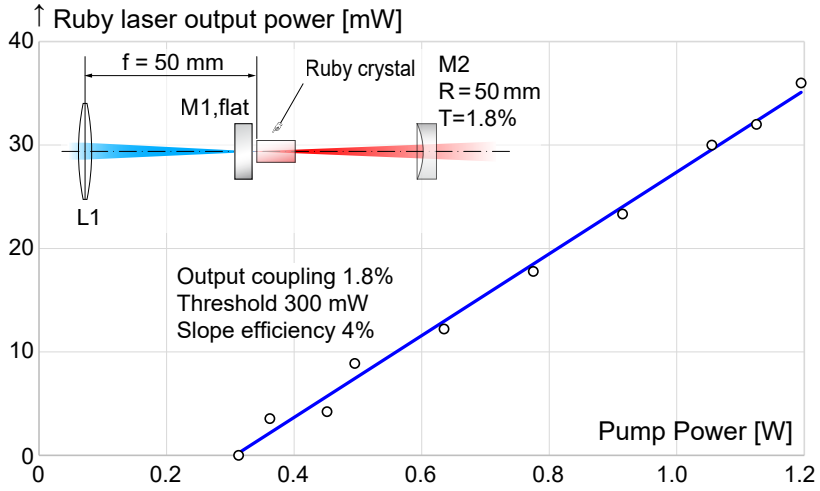

Fig. 6. Ruby laser output power versus pump power for the semi-concentric resonator with an output coupling mirror M2 of 1.8%

versus pump power for the semi-concentric resonator for a mirror M2 with a radius of curvature of 50 mm and an output coupling of about 1.8 % at 694 nm. After raising from threshold at about 300 mW we see an almost linear increase of the output power up to 36 mW with a slope efficiency of 4%. The ruby laser oscillates in a variety of more or less higher order modes, depending on the resonator adjustment. As the laser diode is a transverse multimode laser with an elliptical beam shape (1:3), the focus within the crystal is expected to be elliptical too (modified by the described "channeling" in Fig. 5), while the mode volume of the resonator has cylindrical

OSA CONTINUUM

symmetry. This leads to a mismatch, which favors transversal modes. We found in all cases that the linear polarization of the ruby laser output is independent of the pump laser polarization, but is defined by the rotation angle of the ruby crystal with respect to its axis.

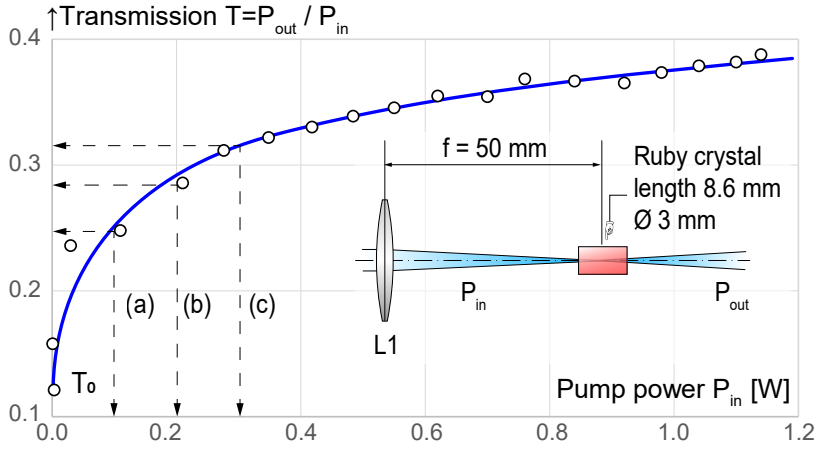

Fig. 7. Ruby crystal transmission versus pump power. (a), (b), (c) correspond to calculated and measured threshold pump powers, used for calculations summarized in Table 1 and discussed below.

With increasing pump power the transmission $T = P_{out}/P_{in}$ (P_{in}: input power, P_{out}: transmitted power) of the pump radiation through the crystal and the absorption within the crystal strongly changes. This can be seen from Fig. 7, where the transmission versus the pump power is given under focusing conditions but without mirrors. At very low pump power ($P_{in} \rightarrow 0$) the transmission reaches a minimum value of T_0 which is given by

$$T_0 = e^{-N_0 \cdot \sigma_p \cdot L} \tag{1}$$

where N_0 is the ground state density of Cr^{3+} ions, σ_p the absorption cross section of the pump radiation and L the crystal length. With $T_0 = 0.12$ (from Fig. 7), $\sigma_p = 2 \cdot 10^{-19} cm^2$ at 405 nm [9] and $L = 8.6\,mm$, a ground state density of $1.23 \cdot 10^{19} cm^{-3}$ can be calculated, in agreement to a Cr^{3+} concentration of about 0.05% for the crystal. With increasing pump power (pump intensity I) the ground state density is reduced and finally population inversion is generated. To calculate the population densities, three level rate equations may be used. With the level numbering of Fig. 1 and assuming a transfer rate from level 3 to level 2 much larger than the spontaneous emission rate from level 2 to 1, the population density in level 3 remains almost zero and we obtain, under steady state condition and for zero ruby laser field, for the population density N_1 (inversion density $\Delta N = N_2 - N_1$; $N_1 + N_2 = N_0$) the following equation:

$$N_1 = \frac{N_o}{1 + I/I_0} \tag{2}$$

where I is the pump intensity and I_0 is given by:

$$I_0 = \frac{h \cdot \nu_p}{\tau \cdot \sigma_P} = 7.01 \cdot 10^2\,[Wcm^{-2}]$$

with τ being the lifetime of the upper laser level ($\tau = 3.5ms$) and σ_p as given above for the pump frequency ν_p. To calculate the transmission (absorption) we have to integrate the intensity change $dI = -I \cdot \sigma_P \cdot N_1(I) \cdot dz$ along the length z of the crystal. As the intensity distribution

OSA CONTINUUM

perpendicular to the z-axis is not well known and itself will depend on z, due to the focusing, the elliptical pump beam and the influence of the "channeling", such a calculation is difficult and out of scope in this work (some aspects are discussed in [7]). Nevertheless, estimates and predictions are possible, assuming constant (average) values for N_1 and ΔN. An estimate of ΔN is obtained by considering the gain G at the laser transition, which is given by

$$G = \sigma_L \cdot L \cdot \Delta N;\ \Delta N = N_2 - \frac{g_2}{g_1} \cdot N_1 \tag{3}$$

for small values of G, where σ_L is the amplification cross section at the laser transition and g_1, g_2 are the degeneracy factors of the lower and upper laser level ($g_2 = 2; g_1 = 4$). For σ_L we take the

Table 1. Data of measurements and calculations

	measured		calculated				
	Threshold pump power	Trans-mission	Densities $10^{18}cm^{-3}$		Gain G	Pump intensity	Pump area P/I
Index*	P[mW]	T (Fig.7)	N_1	ΔN	%	$10^2 W cm^{-2}$	$10^{-4}cm^2$
a	100**	0.24	8.20	0.00	0.0	3.51	2.85
b	200	0.28	7.40	1.20	1.0	4.64	4.30
c	300	0.32	6.62	2.37	2.1	6.00	5.00

Calculated data using (1) - (3); * corresponding to Fig. 7 and text; ** fictitious value for G=0

value of $\sigma_L = 1 \cdot 10^{-20} cm^2$ (c-axis 90° to crystal axis) as given in [9]. In the following three specific pump power situations (a), (b), (c) indicated in Fig.7 are discussed, to compare measured and calculated data summarized in Table 1.

(a) For $\Delta N = 0 (G = 0)$ we obtain for the ground state density $N_1 = N_0/1.5$ and via Eq. 2 for the minimum possible threshold pump intensity $I_a = 3.5 \cdot 10^2 W cm^{-2}$. Using Eq. 1 with N_0 replaced by N_1, a transmission of $T_a = 0.24$ is calculated, which, according to the measured transmission curve in Fig. 7 corresponds to a fictitious threshold pump power of about 100 mW (indicated in Table 1 by **).

(b) For the resonator with high reflective mirrors (Fig. 2) a threshold pump power of 200 mW was measured, which according to Fig. 7, corresponds to a transmission of 0.28. For this transmission corresponding values for N_1 and ΔN (Table 1) are calculated in a similar way, delivering finally a gain of G = 0.01 (1%), which is a very realistic gain to compensate for the losses of a resonator consisting of two mirrors and two crystal surfaces.

(c) For the resonator with an output coupling mirror of about 1.8% (Fig. 6) a threshold pump power of 300 mW was measured. This corresponds to a transmission of 0.32 (Fig. 7), which then yields the values of N_1 and ΔN given in Table 1, leading to a gain of G = 0.021 (2.1%), a bit lower than expected with respect to the additional output coupling losses of 1.8%.

In summary the considered simple model yields a good agreement between measured and calculated data, considering the uncertainties in measuring exact threshold pump powers.

Considering the given intensities, much lower threshold pump powers should be possible by stronger focusing or a better pump beam profile. With increasing pump power, the data of Table 1 show an increase of the pumped area. This increase will be much stronger for the high pump powers, which is indicated by the flattening of the transmission curve (Fig. 7) above the threshold value of 300 mW. The increase of the pumped volume is also directly seen from the fluorescence track. At present an output power of 36 mW is obtained at the maximum pump

OSA CONTINUUM

power of 1200 mW, corresponding to a total conversion efficiency of 3%. In former experiments, with argon ion laser pumping and liquid nitrogen cooling of the ruby crystal, efficiencies of more than 10% have been reported [6]. It is expected that such efficiencies will also be possible with laser diode pumping at room temperature, by beam forming and adequate focusing of the laser diode, a matching of the pump and mode volume and by optimization of the output coupling. It should be noted, that during our experiments a patent appeared, claiming the laser diode pumping of ruby [10].

2.2. Operation of a cw ruby ring laser

The narrow linewidth of ruby should allow the generation of highly coherent radiation. To realize this, single frequency operation will be necessary, which can best be achieved by using a ring resonator, where traveling waves avoid spatial hole burning, mainly responsible for multimode emission in standing wave resonators. The spectral properties of pulsed ring ruby lasers have been investigated and single frequency emission has been reported [11], but to the best of our knowledge cw operation of a ruby ring laser has not been demonstrated so far. Our experimental setup is shown in Fig. 8. The ruby ring laser is arranged as a bow tie resonator to compensate

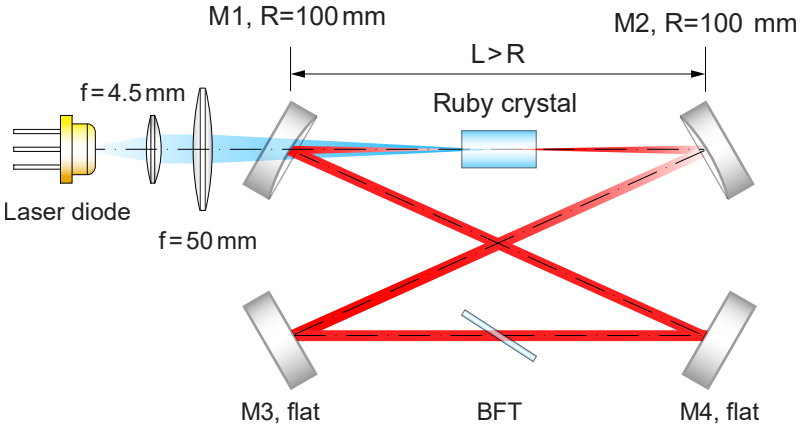

Fig. 8. Setup of the ruby ring laser with birefringent tuner (BFT). Resonator length about 450 mm.

for astigmatic aberrations and to realize a compact system with small angles of incident at the mirrors. The ruby crystal is located in the center between the curved mirrors (R=100 mm) M1 and M2 and is pumped via the mirror M1 (90% transmission at 405 nm, high reflectivity at 694 nm; all other mirrors have high reflectivity at 405 nm and 694 nm) with the same laser diode as used for the linear resonator. The ruby ring laser operates in clockwise and counterclockwise direction with a threshold of 200 mW. With an inserted plan-parallel quartz plate for output coupling an output power of 10 mW for each direction was obtained at a pump power of 1.2 W. The emission contains low order transverse modes. Spike free operation is achieved within 4 ms after switching on the pump laser diode and is almost noise free (Fig. 9). Normally, the ring oscillates on both R lines, but with an internal birefringent tuner (BFT) operation on a single line is possible. By suitable alignment of the resonator and especially by insertion of a pinhole between mirrors M3 and M4 transversal modes can fully be removed, and first measurements with an external Fabry-Perot give strong evidence for single frequency emission. It is expected, that under these conditions a line width in the range of 100 Hz will be possible, but this has to be investigated further in more detail. For clean conditions of such investigations an internal optical diode will be necessary to obtain unidirectional oscillation (as demonstrated in [11]) and suppress unwanted competition between clockwise and counter-clockwise oscillation.

OSA CONTINUUM

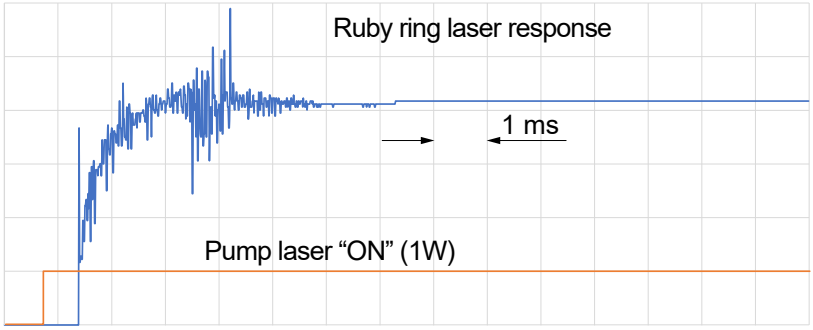

Fig. 9. Transient response of the ruby ring laser.

3. Summary and conclusions

First detailed investigations on a 405 nm diode pumped cw ruby laser operating at room temperature are reported. With a semi-concentric resonator a threshold of 200 mW and an output power of 36 mW at 1.2 W pump power are obtained at present. Investigations and calculations indicate, that much lower thresholds and higher output powers will be possible with the discussed optimizations. For the first time a cw diode pumped ruby ring laser is demonstrated, which will allow highly coherent single frequency oscillation. Furthermore, we succeeded to pump the cw ruby laser in the same resonator configurations with a 445 nm laser diode with thresholds around 400 mW. Such 445 nm laser diodes are of interest, since output powers of more than 5 W are available at low costs.

The tiny ruby crystal and the small pump laser diode (TO-9 housing) will allow the realization of very compact laser systems. Such systems may be of interest in laser medicine, eye treatment and biophotonics, where a high penetration depth in living matter is required or for laser metrology and space applications, where highly coherent laser emission is needed.

Looking back into laser history, Maiman’s famous ruby laser initiated a fascinating development, which also led to the invention of the powerful tiny laser diode used here to pump the ruby laser, allowing now compact and low cost laser setups, well suited for demonstration and education purposes, as well as for scientific applications.

References

1. T. H. Maiman, “Stimulated optical radiation in ruby,” Nature **187**, 493 (1960).
2. T. H. Maiman, “Optical and microwave-optical experiments in ruby,” Phys. Rev. Lett. **4**, 564 (1960).
3. D. F. Nelson and W. S. Boyle, “A continuously operating ruby optical maser,” Appl. Opt. **1**, 99 (1962).
4. D. Roess, “Analysis of room temperature cw ruby lasers,” IEEE J. Quantum Electron. **2**, 105 (1966).
5. M. Birnbaum, P. H. Wendzikowski, and C. L. Fincher, “Continuous-wave nonspiking single-mode ruby lasers,” Appl. Phys. Lett. **16**, 436 (1970).
6. T. N. Venkatesan and S. L. McCall, “cw ruby laser pumped by a 5145$\AA$ argon laser,” Rev. Sci. Instrum. **48**, 539 (1977).
7. R. S. Afzal, W. P. Lin, and N. M. Lawandy, “Experimental study of the dynamics of a ruby laser pumped by a cw argon-ion laser,” J. Opt. Soc. Am. B **6**, 2348 (1989).
8. D. E. McCumber and M. D. Sturge, “Linewidth and temperature shift of the *R* lines in ruby,” J. Appl. Phys. **34**, 1682 (1963).
9. D. C. Cronemeyer, “Optical absorption characteristics of pink ruby,” J. Opt. Soc. Am. **56**, 1703 (1966).
10. W. F. Krupke, “GaN pumped ruby laser," US patent 20180041002 (February 8, 2018).
11. L. S. Kornienko, N. V. Kravtsov, N. I. Naumkin, and A.M. Prokhorov, “Single mode ruby ring laser,” Soviet Physics JETP **31**, 290 (1970).